

Effect of boundary conditions and turbulence model on wake around 3D underwater obstacle

Aditya Paspunurwar

Department of Mechanical Engineering

Indian Institute of Technology, Bombay

Abstract

In this project the effect of wake of an underwater obstacle due to different boundary conditions (No slip and Hybrid) as well as different turbulence models available in OpenFOAM is studied. Generally, turbulence modelling is very computationally expensive as it involves capturing small scale eddies. However, in this project the difference in the results for low resolution grids to that of very fine mesh used for LES models are being studied. The results of two different turbulence models: $k-\epsilon$ and SGS Smagorinsky model are compared with each other and experimental data. In addition to this the same turbulence model and flow conditions are applied to a square pyramidal object and results are compared for both the cases.

1. Introduction

The fluid dynamics due to the topography in ocean bed dynamics has received significant attention in the previous years. The impinging flow experience drag due to the momentum transported by topographic internal waves and the turbulent mixing is obtained from the energy conversion from the flow to internal waves. Along with internal waves, wakes are also generated as the flow separates at 3D juncture.

2. Problem Statement

The objective of this project is to study the effect of different boundary conditions and turbulence models on the wake around an obstacle. The domain to study is a cuboid with dimensions $D = 2$, $h = 0.6$, $Lx^- = 6$ (3D), $Lx^+ = 28$ (14D), $Ly = 12$ (6D) and $Lz = 12$ (20h).

Fluid is entering the domain from the inlet with a fixed velocity of $(U_0, 0, 0)$. The viscosity of the fluid is taken as 10^{-6} and Reynolds number of the flow is set as 15000. Figure 1 shows a crude view of computational domain.

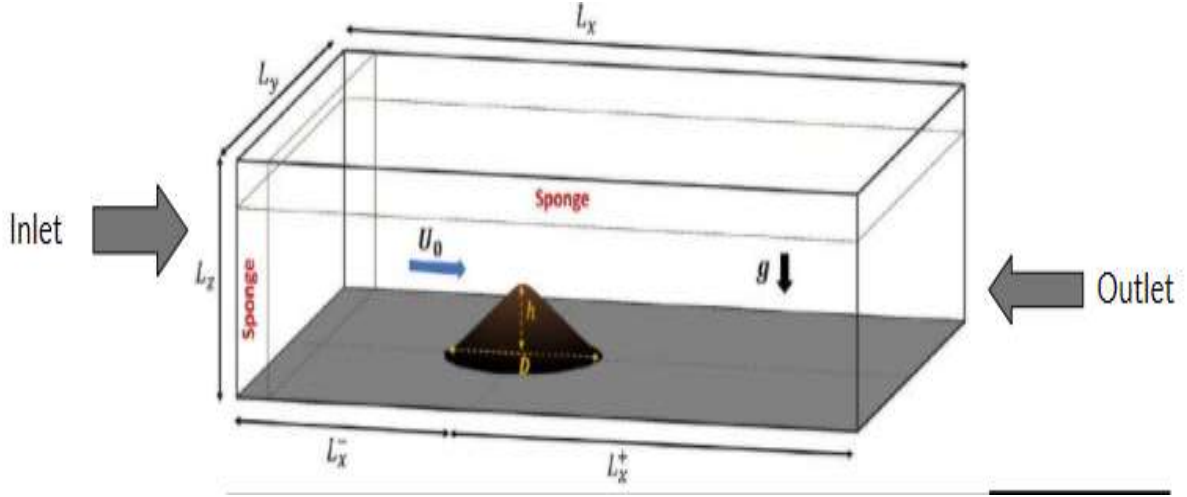


Figure 1: Domain of Study (Picture taken from Puthan et.al)

3. Governing Equations

The following set of equations are being solved using buoyantBoussinesqSimpleFoam.

Navier-Stokes Equations:

$$\frac{\partial u_i}{\partial x_i} = 0$$

$$\frac{\partial u_i}{\partial t} + u_j \frac{\partial u_i}{\partial x_j} = \frac{-1}{\rho_0} \frac{dp}{dx_i} - g\delta_{i3} + \frac{\partial \tau_{ij}}{\partial x_j}$$

Here u denotes the velocity, p is the pressure, τ is the stress tensor and δ is Kronecker's delta function.

k- ϵ model:

$$\frac{D}{Dt}(\rho k) = \nabla \cdot (\rho D_k \nabla k) + P - \rho \epsilon$$

$$\frac{D}{Dt}(\rho \epsilon) = \nabla \cdot (\rho D_\epsilon \nabla \epsilon) + \frac{C_1 \epsilon}{k} \left(P + C_3 \frac{2}{3} k \nabla \cdot U \right) - C_2 \rho \frac{\epsilon^2}{k}$$

$$\nu_t = C_\mu \frac{k^2}{\epsilon}$$

Here k is the turbulent kinetic energy, ε the specific dissipation rate, P is the production term, D_k and D_ε are the effective diffusivity for respective equations and ν_t is the turbulent viscosity. The default value of the coefficient C_1 , C_2 , C_3 and C_μ are used here.

Smagorinsky Sub Grid Scale model:

$$\tau_{ij} = \frac{2}{3}k_{sgs}\delta_{ij} - 2\nu_{sgs}dev(\bar{D})_{ij}$$

$$\bar{D}_{ij} = \frac{1}{2}\left(\frac{d\bar{u}_i}{dx_j} + \frac{d\bar{u}_j}{dx_i}\right)$$

$$k_{sgs} = \frac{1}{2}\tau_{kk} = \frac{1}{2}(\overline{u_k u_k} - \bar{u}_k \bar{u}_k)$$

$$\nu_{sgs} = C_k \Delta \sqrt{k_{sgs}}$$

Here C_k is a model constant whose default value 0.094 is used in this study. Apart from this D is the resolved scale strain rate tensor, ν_{sgs} is the sub-grid scale viscosity, k_{sgs} is the sub-grid scale kinetic energy and Δ is the grid size that defines sub-grid length scale.

4. Simulation Procedure

There are three folders in the case folders namely 0, constant and system. 0 directory consists the initial values of various fields such as U , p , p_rgh , k , ε etc. In the constant directory we provide the transport and turbulence properties of the system, whereas we can specify different schemes and controlling parameters in the system folders. For all the simulations in this project buoyantBoussinesqSimpleFoam. Since both temperature and density is not a variant in this case thus β (thermal expansion coefficient) is set as 0 and T is set same as T_{ref} . Thus this solver is steady, incompressible and turbulent solver. The table below shows the fluid properties and turbulence parameters:

| Variable | Value | Units |
|----------------------------------|------------------|--------------------------------|
| Density (ρ) | 1 | kgm ⁻³ |
| Kinematic Viscosity (ν) | 10 ⁻⁶ | m ² s ⁻¹ |
| Laminar Prandtl Number (Pr) | 10 ¹⁰ | Dimensionless |
| Turbulent Prandtl Number (Prt) | 10 ¹⁰ | Dimensionless |
| Turbulent kinetic energy (k) | 10 ⁻⁸ | m ² s ⁻² |

| | | |
|--|------------------------|---------------------------|
| Turbulent dissipation energy (ε) | $2.032 \cdot 10^{-14}$ | m^2s^{-3} |
| Turbulent Intensity (I) | $3.44 \cdot 10^{-4}$ | % |
| Turbulent Mixing length (L) | 0.14 | m |

Table 1: Properties of Fluid and turbulence properties

The Prandtl number is as set very high in order to make α very low so that there is no change in temperature.

4.1 Geometry and Mesh

External meshing software Salome was used to generate different mesh for this project. The computational domain is shown in Figure 2. Only tetrahedral elements are used for structured meshing and the grid is refined near the bottom wall and obstacle wall for capturing viscous sub layer. It is a 3 dimensional mesh with around 150k cells. The domain is 34m in length and 12m in breadth as well as height. Figure 3 highlights the bottom face where the cone is kept, whereas Figure 4 is the magnified view of the mesh near the cone (obstacle).

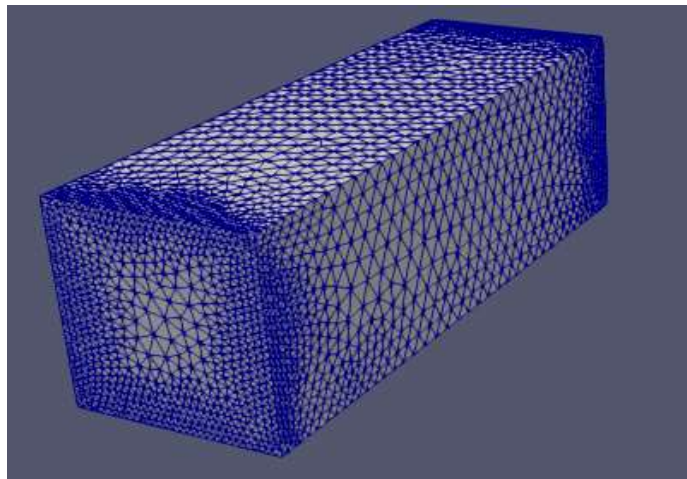


Figure 2: Orthographic view of domain

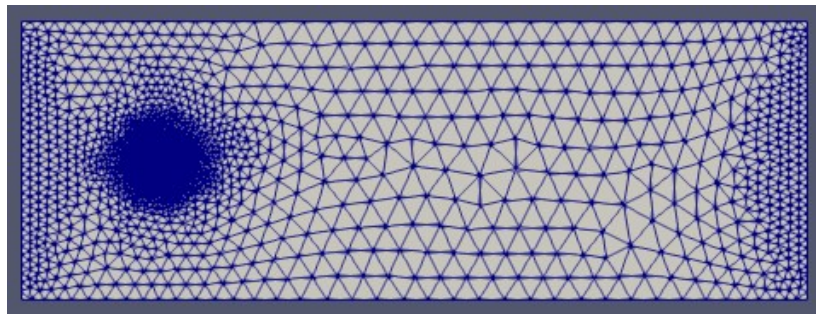


Figure 3: Bottom face

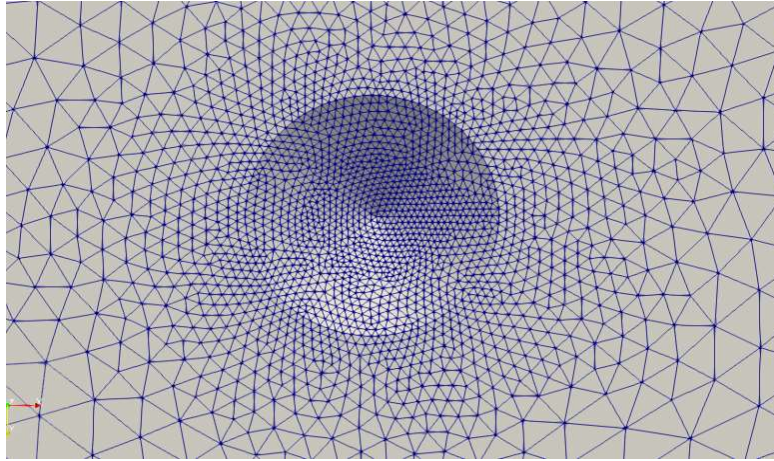


Figure 4: Enlarged view of conical surface

Grid Independence Study:

A mesh sensitivity analysis is carried out to obtain most optimal results with minimum number of cells in order to reduce computational cost. Three non-uniform structured meshes with tetrahedral elements were generated with 110k, 130k and 180k cells. Figure 3 below shows the variation of U_x/U_o with length along the x-axis exactly behind the obstacle at $z = 0.3$ and $y = 0$ where U_o is the fixed inlet velocity. It can be seen that the meshes with 130k and 180k cells are almost similar. Also it should be noted that for the sensitivity analysis mesh has not been refined near the walls because of large computational expense.

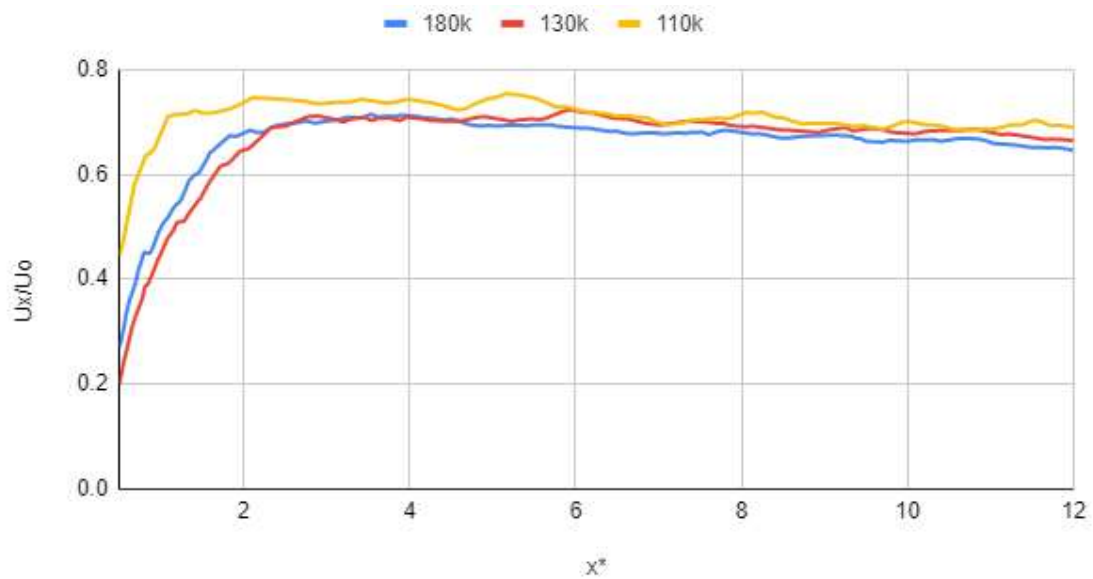


Figure 5: Grid Independence Study

4.2 Initial and Boundary Conditions

The faces of this domain are set as inlet, outlet, frontAndBack, top which are patches along with cone and bottom both of which are walls.

➤ **Velocity (U) ms⁻¹:**

Inlet: Fixed Value – uniform (7.5×10^{-3} , 0, 0)
 Outlet: Zero Gradient
 Cone: no Slip
 Bottom: no Slip or slip (for hybrid)
 FrontAndBack: Fixed Value – uniform (7.5×10^{-3} , 0, 0)
 Top: Fixed Value – uniform (7.5×10^{-3} , 0, 0)
 Internal Field: uniform 0

➤ **Hydrostatic pressure (p_rgh) m²s⁻²:**

Inlet: FixedFluxPressure
 Outlet: Fixed Value (Uniform 0 pressure)
 Cone: FixedFluxPressure
 Bottom: FixedFluxPressure
 FrontAndBack: FixedFluxPressure
 Top: FixedFluxPressure

➤ **Kinematic pressure (p) m²s⁻²:**

Inlet: Calculated (Value uniform 0)
 Outlet: Calculated (Value uniform 0)
 Cone: Calculated (Value uniform 0)
 Bottom: Calculated (Value uniform 0)
 FrontAndBack: Calculated (Value uniform 0)
 Top: Calculated (Value uniform 0)

➤ **Turbulent kinetic energy (k) m²s⁻²:**

InternalField: = 10^{-8}
 Inlet: turbulentIntensityKineticEnergyInlet (intensity value = 3.44×10^{-4})
 Outlet: Zero Gradient
 Cone: kqRWallFunction
 Bottom: kqRWallFunction
 FrontAndBack: Zero Gradient
 Top: Zero Gradient

➤ **Turbulent dissipation rate (epsilon) m^2s^{-3} :**

InternalField: $2.032 \cdot 10^{-14}$

Inlet: turbulentMixingLengthDissipationRateInlet (mixing length - 0.14)

Outlet: Zero Gradient

Cone: epsilonWallFunction

Bottom: epsilonWallFunction

FrontAndBack: Zero Gradient

Top: Zero Gradient

➤ **Kinematic Eddy Viscosity (nut) m^2s^{-1} :**

Inlet: Calculated (Value uniform 0)

Outlet: Calculated (Value uniform 0)

Cone: nutkWallFunction

Bottom: nutkWallFunction

FrontAndBack: Calculated (Value uniform 0)

Top: Calculated (Value uniform 0)

➤ **Hybrid BC:**

Bottom: Slip velocity

Cone: No-slip velocity

➤ **No-slip BC:**

Bottom: No-slip velocity

Cone: No-slip velocity

4.3 Solver

The solver used for running the simulations is buoyantBoussinesqSimpleFoam. Few modifications have been done in order to switch off the energy equation and calculation of turbulent kinetic energy in SGS modelling. This solver is used instead of simpleFoam in order to incorporate the gravity term.

Solver Validation:

The modified solver is tested against simpleFoam for the cases of flow inside a pipe using k- ϵ model. For the modified solver gravity term is set as 0.

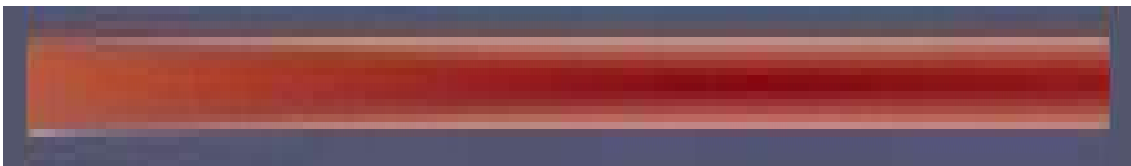


Figure 6: velocity profile - buoyantBoussinesqSimpleFoam

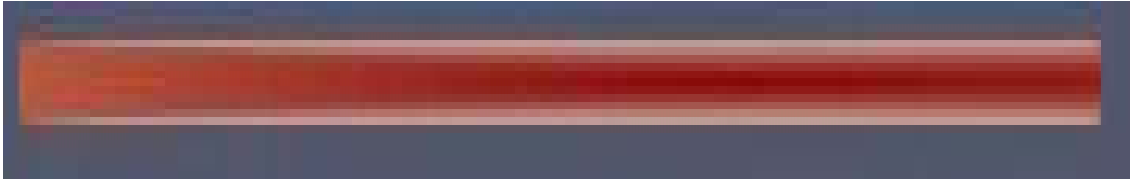
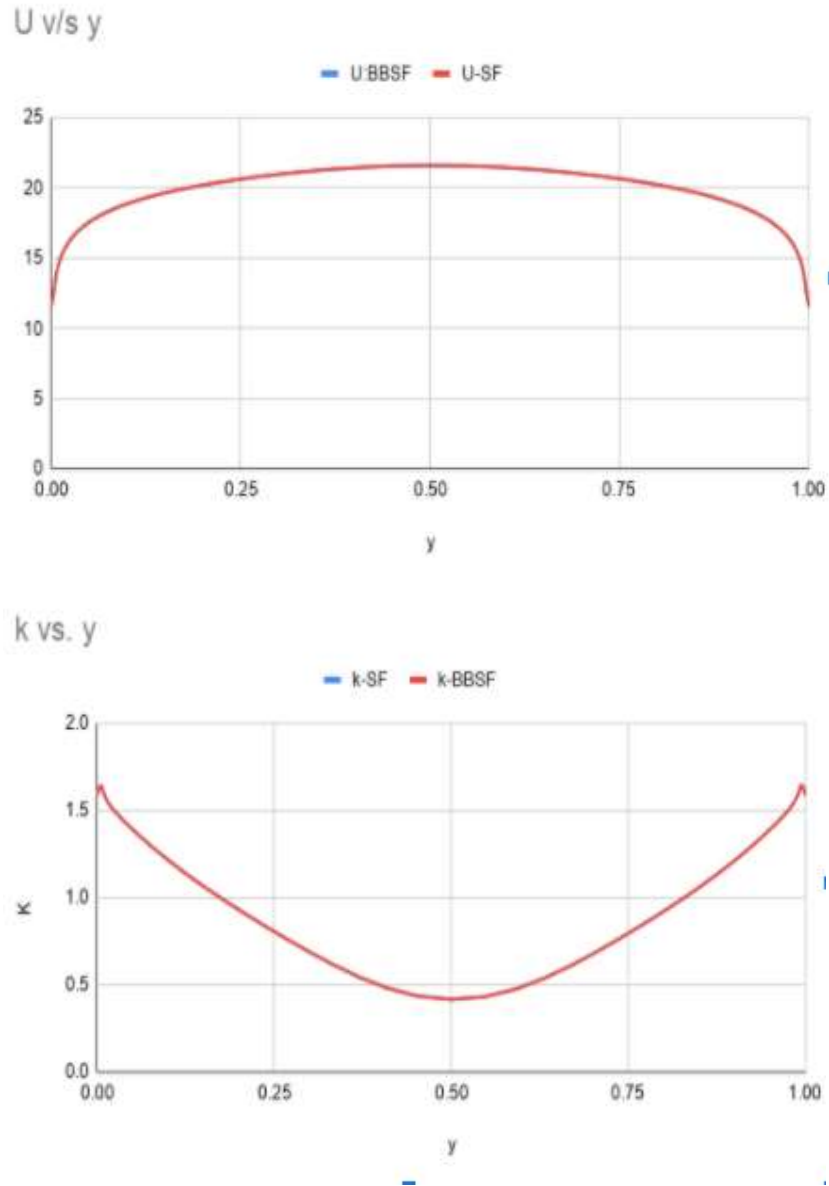


Figure 7: velocity profile - simpleFoam



As it can be seen from the above two graphs that the velocity and turbulent kinetic energy are exactly equal to each other. Thus the modified solver is working fine.

5. Results and Discussions

As mentioned earlier that the simulations have been performed using buoyantBoussinesqSimpleFoam solver for both turbulence models. The initial comparisons are qualitative comparison of contours with each other and experimental data followed by quantitative comparisons.

5.1 Qualitative Comparison of Contours:

In the following section the contours of velocity in x and z directions are plotted in various planes and are compared with experimental data. Please note that in the experiments density was varying due to Brunt-Vaisala frequency, whereas in this project density is kept as constant. Hence the ripples present in the experimental contours will not be present in the measured contours. These contours are produced for the mesh with 152280 cells for which the value of average y^+ for the bottom wall is 5.78 and for cone is 1.31. Thus the k-epsilon model is unable to accurately predict the turbulence characteristics. Each simulation is being run for 30000s with a time step of 10s. Mean value is measured from $t = 18000$ to $t = 30000$ wherever it is present. All the experimental contours are taken from *Puthan et al.*

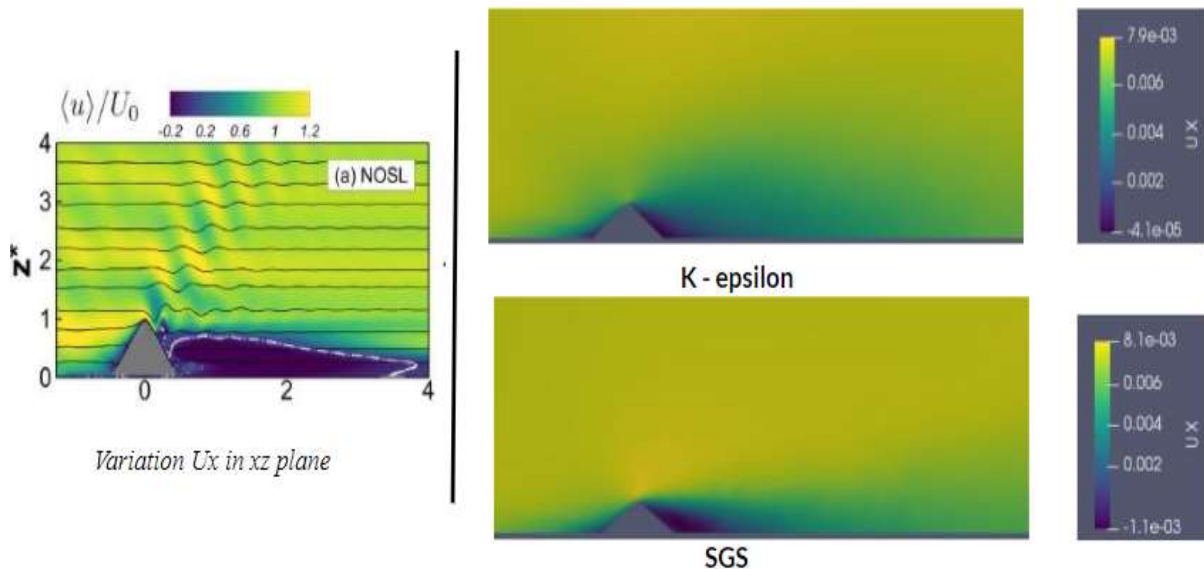


Figure 8.1: Variation of U_x in x-z plane at $y=0$ for no-slip case

From the figure 8.1 it can be seen that apart from the ripple effect, SGS is more closely able to produce the wake effect than k- ϵ model. In k- ϵ the velocity is diverging and is spreading out because of the low y^+ value.

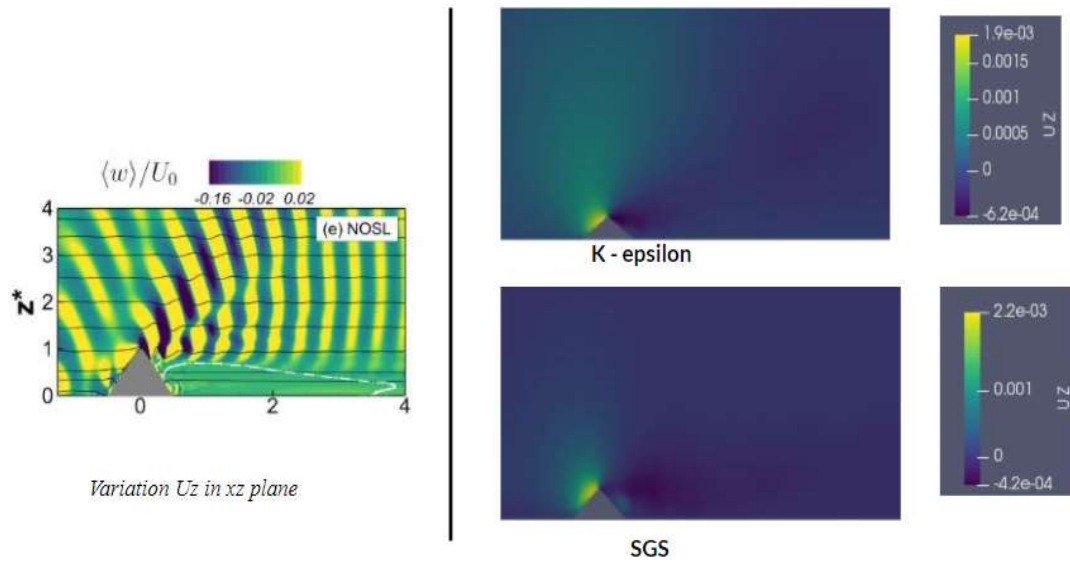


Figure 8.2: Variation of U_z in x-z plane at $y=0$ for no-slip case

Figure 8.2 shows that both SGS model and $k-\epsilon$ model are producing almost similar results which are considerably different than the experimental ones due to absence of density equation¹.

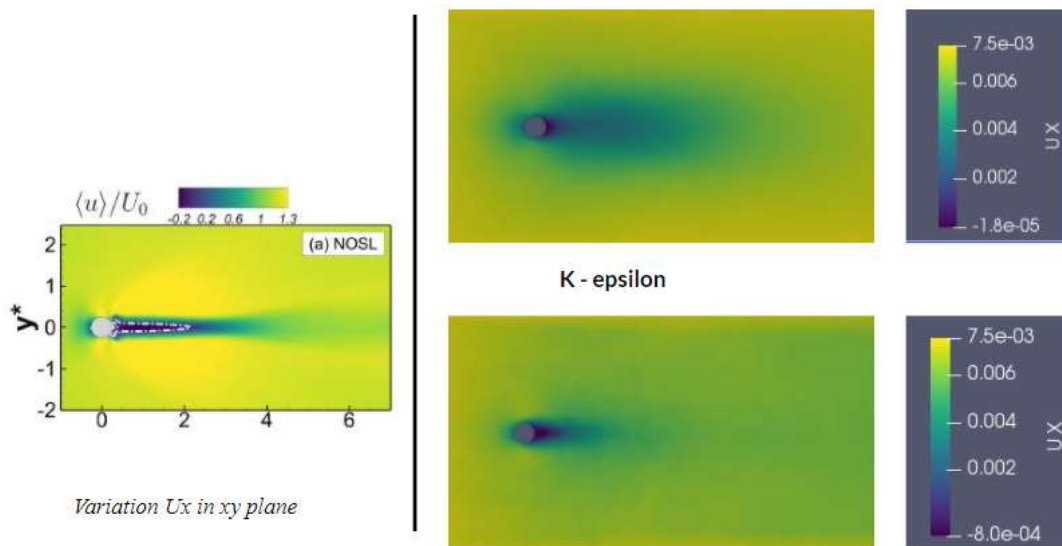


Figure 8.3: Variation of U_x in x-y plane at $z^*=0.5$ for no-slip case

From the figure 8.3 it can be seen that SGS has more well-defined wake behind the obstacle than $k-\epsilon$ model.

¹ Density Equation: $\frac{\partial \rho}{\partial x} + u_j \frac{\partial \rho}{\partial x_j} = \frac{dX_j}{dx_j}$ where X is the density flux vector

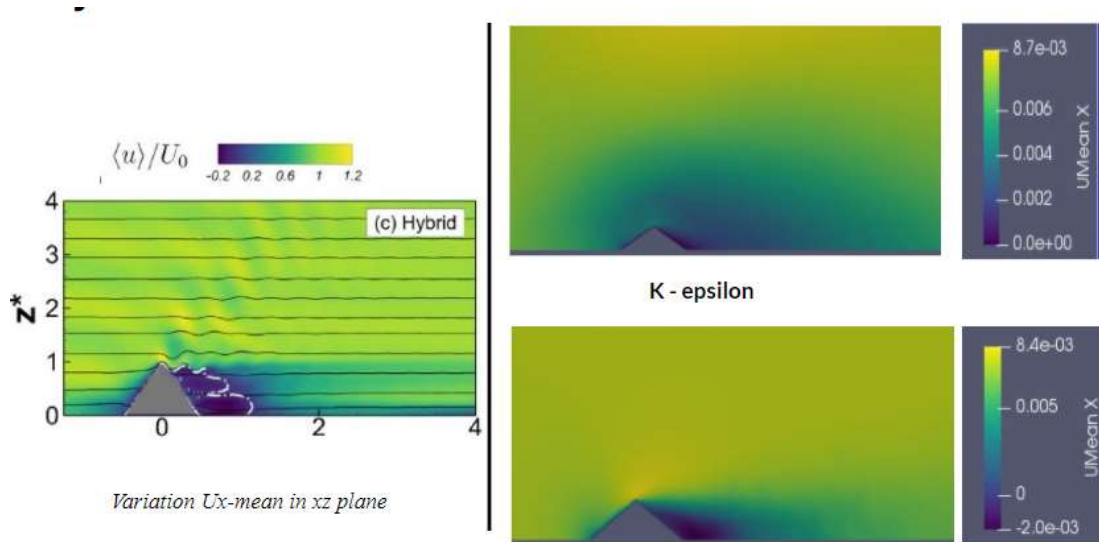


Figure 8.4: Variation of mean- U_x in x-z plane at $y=0$ for hybrid case

It can be seen from figure 8.4 that k- ϵ model is not able to converge the velocity for it to be below the tip of cone. On the other hand, SGS model predicts very closely to the experimental results.

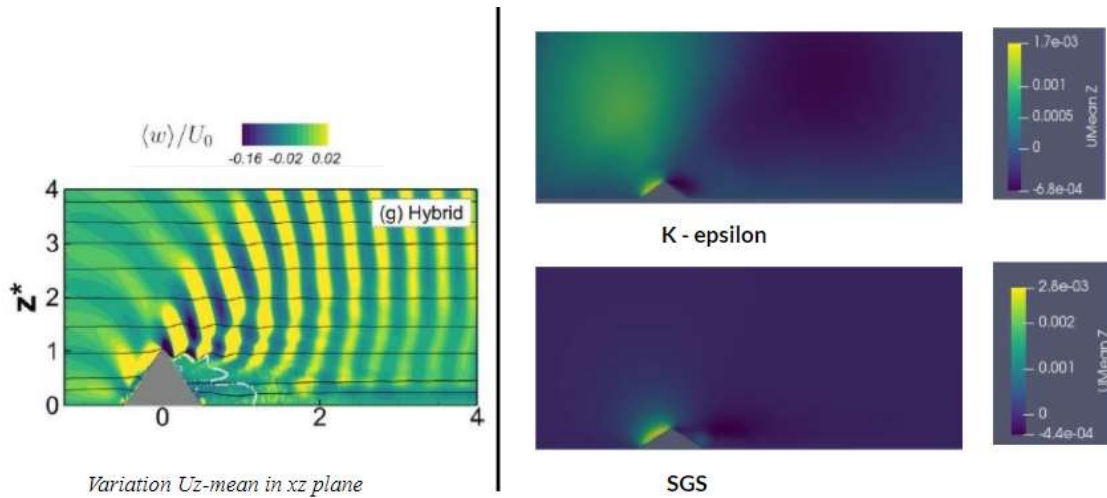


Figure 8.5: Variation of mean- U_z in x-z plane at $y=0$ for hybrid case

It can be seen from figure 8.5 that both k- ϵ model and SGS model produce significantly different result that the experimental one. However, it can be seen that the velocity profile behind the obstacle is more accurately captured by SGS model.

5.2 Parametric Analysis

U_d/U_o v/s x^* (No slip)

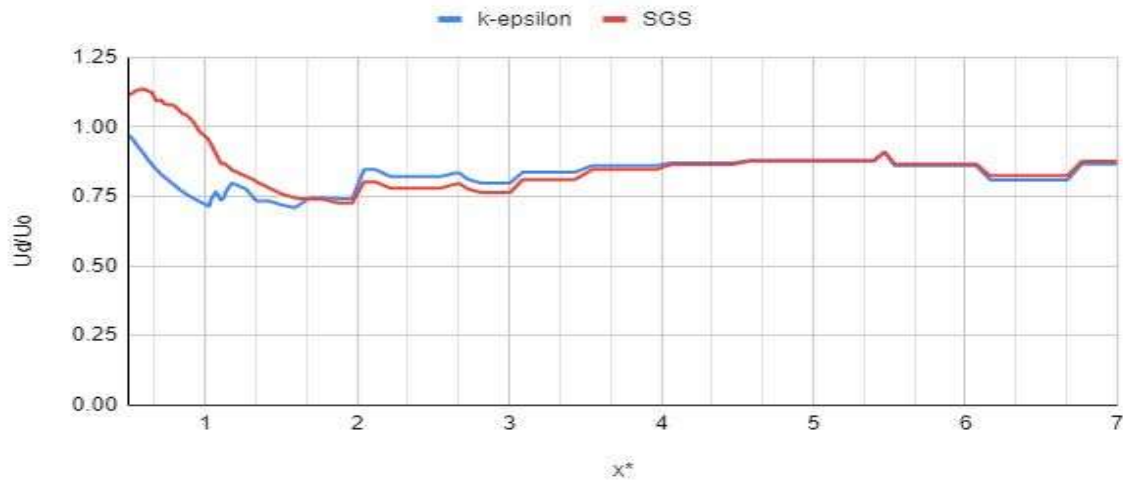


Figure 9.1

U_d/U_o v/s x^* (Hybrid)

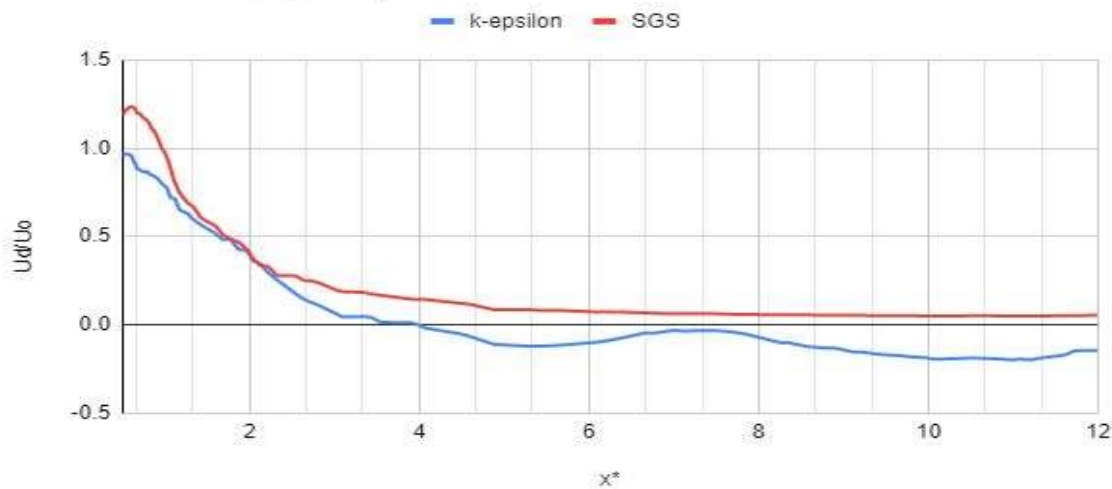


Figure 9.2

In figure 9.1 and 9.2 the variation of defect velocity ($\langle u(x, y, z, t) \rangle - U_o$, where $\langle \rangle$ denotes averaging of the given value) with x behind the obstacle is plotted at $y^* = 0$ and $z^* = 0.25$. It can be inferred from the figures that for both cases the defect velocity is initially high and reduces to a steady value which is more for no-slip case. This is due to the fact that because of no-slip velocity at wall is low and to balance momentum conservation velocity should be higher than U_o away from the wall.

5.3. Qualitative Results for square pyramidal obstacle:

For the following results the conical obstacle is replaced with square pyramidal obstacle. The number of tetrahedrons in the mesh are 112827. y^+ for the k- ϵ model is above 10 for this case.

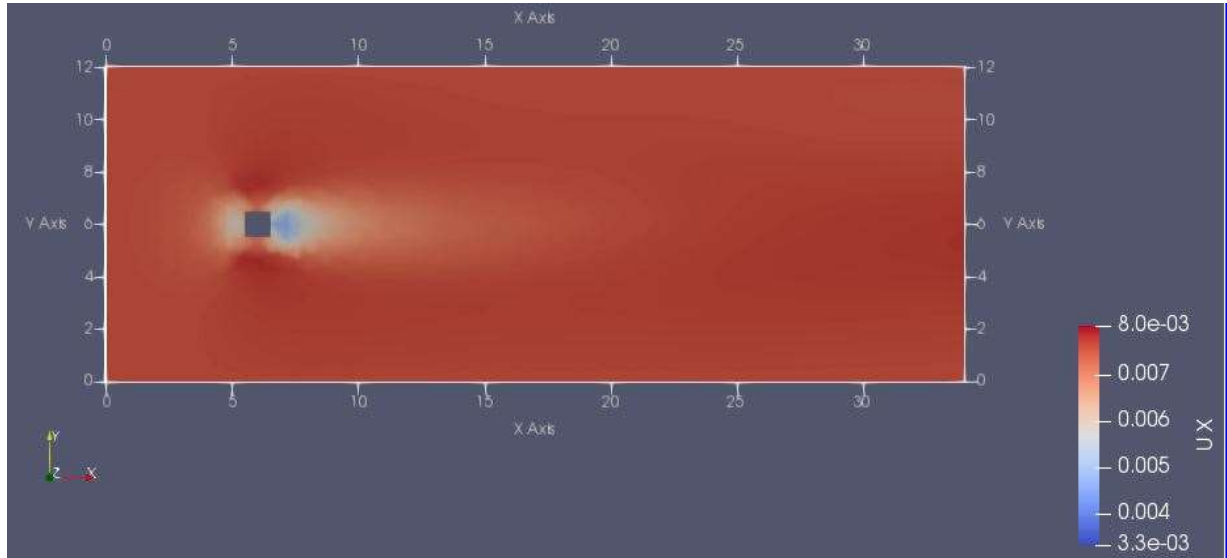


Figure 10.1: Variation of U_x in x-y plane for k- ϵ model (No-slip)

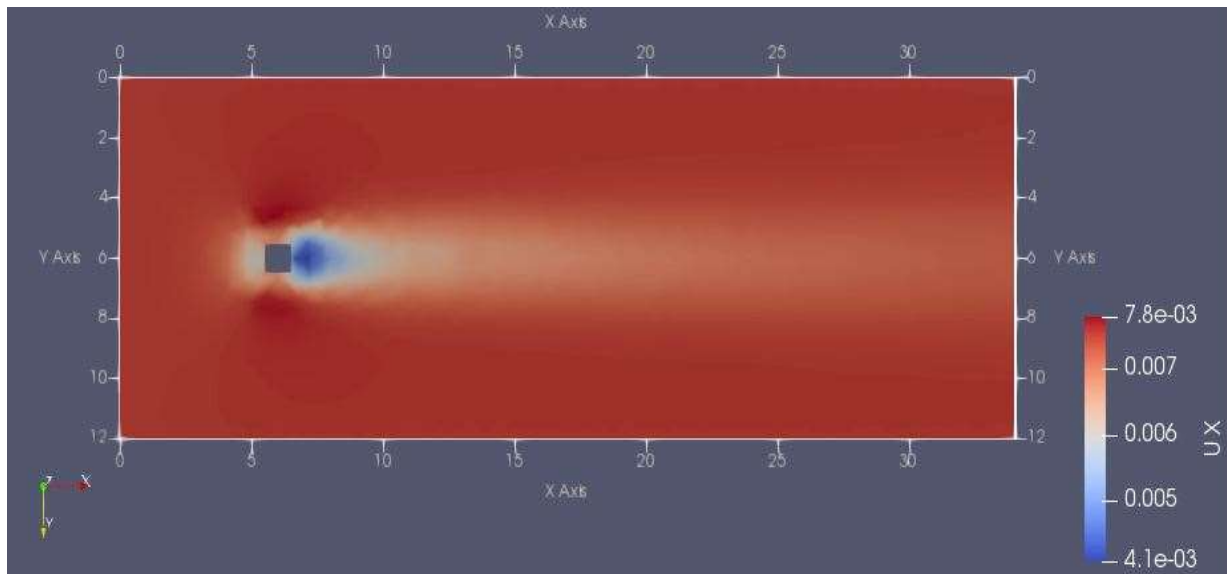


Figure 10.2: Variation of U_x in x-y plane for SGS Smagorinsky model (No-slip)

From the above results it can be notably seen that the wake behind square pyramid is more divergent in comparison to that produced behind cone.



Figure 11.1: Variation of U_x in x-z plane for k- ϵ model (No-slip)



Figure 11.2: Variation of U_x in x-z plane for SGS model (No-slip)



Figure 11.3: Variation of U_z in x-z plane for k- ϵ model (No-slip)



Figure 11.4: Variation of U_z in x-z plane for SGS model (No-slip)

From figure 11.1 and 11.2 it can be seen that both models produce almost similar results. Also in case of figure 11.3 and 11.4 the variation of U_z is coherent for both the cases. Moreover we can see that U_z is almost constant everywhere except near the walls of the obstacle.

5.4. Parametric Analysis of square pyramid case:

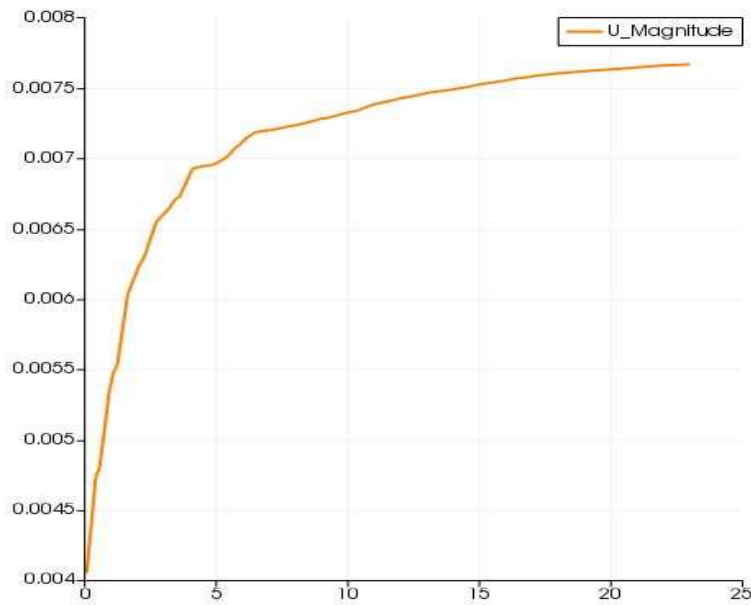


Figure 12.1: Variation of $|U|$ in x axis behind the obstacle at $y^*=0$ and $z^*=0.25$ ($k-\epsilon$)

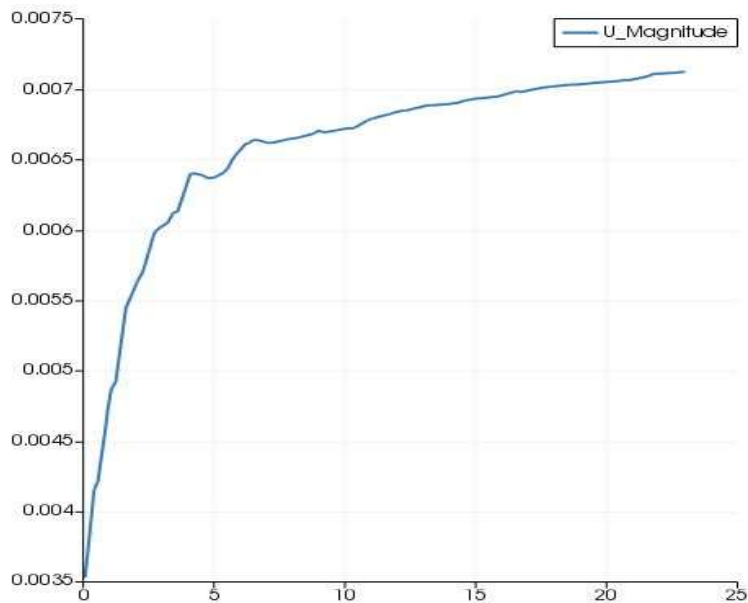


Figure 12.2: Variation of $|U|$ in x axis behind the obstacle at $y^*=0$ and $z^*=0.25$ (SGS)

It can be inferred from the above plots $U_Magnitude$ for $k - \epsilon$ model is greater than SGS model. However, both the models follow the same trend starting from a small value and finally achieving a steady value. $U_Magnitude$ for $k - \epsilon$ is higher because the simulation has not converged in 30000 timesteps whereas SGS model has converged before that.

Conclusions:

In this this project, we simulated turbulent flow through a domain inside the ocean with an obstacle sitting on the bed using two different turbulence models. The performance of the different turbulence models is compared with each other and experimental results using different parameters such as defect velocity, velocity and T.K.E. The $k - \epsilon$ model was observed to not predict the accurate results because y^+ value is less than 11 and the simulation did not converge with 30000 time steps. On the other hand, SGS model was found to converge faster and give better results. Thus it can be concluded from the project that y^+ is a major factor for $k-\epsilon$ model and should be kept above 11 in order to achieve accurate results. In addition to this SGS model can predict better results if one provides more grid resolution.

Reference

- P. Puthan, M. Jalali, J.L. Ortiz-Tarin et al., The wake of a three-dimensional underwater obstacle: Effect of bottom boundary conditions, *Ocean Modelling* 149 (2020) 101611
- Wang et. al, LES study on the shape effect of ground obstacles on wake vortex dissipation, *Aerospace Science and Technology*
- Shang, Y.: A Two-equation SGS model tutorial. *Proceedings of CFD with OpenSource Software, 2017*, Edited by Nilsson. H. ,http://dx.doi.org/10.17196/OS_CFD#YEAR_2017
- Master's Thesis of Mari Vold: Three-dimensional Numerical Modeling of Water Flow in a Rock-Blasted Tunnel, 2017